JOURNAL OF AGRICULTURAL AND FOOD CHEMISTRY

Photostability of Kainic Acid in Seawater

JUSTINA M. BURNS,[†] TRACEY B. SCHOCK,[‡] MICHELLE H. HSIA,[‡] PETER D. R. MOELLER,[‡] AND JOHN L. FERRY*,[†]

Department of Chemistry and Biochemistry, University of South Carolina, Columbia, South Carolina 29208, and Coastal Center for Environmental Health and Biomolecular Research, Charleston, South Carolina 29412

The environmental degradation of a mixture of domoic acid (DA) and kainic acid (KA) in seawater with and without added transition metals is reported. The association constants for kainic acid with Fe^{III} and Cu^{II} were determined using ^1H nuclear magnetic resonance (NMR; $K_{1,Fe^{III}} = 2.27 \times 10^{12}$, $K_{2,Fe^{III}} = 8.99 \times 10^8$, $K_{1,Cu^{II}} = 1.38 \times 10^{10}$, and $K_{2,Cu^{II}} = 4.35 \times 10^7$). The photochemical half-life of kainic acid has been determined to be significantly longer (40–100 h) than that of domoic acid in corresponding marine systems (12–34 h). The significance of this finding was highlighted by a comparison of the quantification of a mixture of kainic and domoic acids during photodegradation by liquid chromatography–tandem mass spectrometry (LC–MS/MS) techniques and the widely used competitive enzyme-linked immunosorbent assay (cELISA; Biosense Laboratories) method. The MS-based analysis showed that approximately 50% of the DA was photodegraded within 15 h. In contrast, the domoic acid cELISA assay reported that the concentration essentially remained unchanged over this period. The possibility of interference from naturally occurring kainic acid during cELISA measurements could lead to the overestimation of total domoic acid, especially if they occur in mixtures in sunlit waters.

KEYWORDS: Kainic acid; iron (III); copper (II); domoic acid; NMR; direct cELISA; LC–MS/MS; ligand-to-metal charge transfer; photodegradation; ligand

INTRODUCTION

Kainic acid (KA) and domoic acid (DA; **Figure 1**) are neurologically active natural products that belong to the kainoid family, which are among the toxins associated with red tides. KA and DA are coproduced by at least three varieties of marine algae (*Digenea simplex*, *Vidalia obtusiloba*, and *Chondria armata*) (*1, 2*). The mode of toxicity for both toxins is through binding to glutamate receptors in the brain (*2–5*). DA is 20–30 times more toxic than KA (per mass), but KA can also induce acute toxicity, with symptoms ranging from seizures to memory effects (*2, 6–8*). Human exposure can result from direct ingestion of the algae and through consumption of tainted seafood (*3–5*). Seafood has two main contamination routes (1) uptake of contaminated particulates by filter feeders, such as shellfish (i.e., clams, mussels, etc.), and (2) subsequent trophic transfer that may lead to human contamination (*5, 9–11*).

Recent studies of the photostability of domoic acid have shown that its complexation by Fe^{III} can lead to rapid photodegradation in sunlit waters (*12–14*). Although the environmental persistence of domoic acid has been researched in depth, the fate of the kainoid family, in general, has not (*9, 12, 15–17*). This in conjunction with the knowledge that domoic acid is not persistent under most environmental conditions raises the question of the photopersistence of kainic acid (*12*).

This paper explores the environmental degradation of kainic acid, with an emphasis on the mechanisms associated with domoic acid degradation (through transition-metal complexes or other components of natural waters, such as NO_3^-, DOM, and PO_4^{3-}) (*13, 16, 18–23*). NO_3^-, DOM, and PO_4^{3-} were selected on the basis of multiple environmental measurements (*13, 16, 18–24*), and their ranges make the subsequent experimentation broadly applicable. Liquid chromatography–tandem mass spectrometry (LC–MS/MS) was used to quantify both KA and DA. These results were correlated with the commercially available competitive enzyme-linked immunosorbent assay (cELISA) for DA.

MATERIALS AND METHODS

Materials. Barnstead E-pure water (18 MΩ cm) was used for all solutions. Instant Ocean from Aqua Systems, Inc. (for composition, please see Supplementary Table 1 in the Supporting Information) was used for simulating seawater after purification by C18 silica to remove trace phthalates, while freeze-dried Suwanee River natural organic matter (1R101N) was purchased from the International Humic Substances Society (for analysis and prep data, please see Supplementary

* To whom correspondence should be addressed: Department of Chemistry and Biochemistry, University of South Carolina, Columbia, SC 29208. Telephone: (803) 777-2646. Fax: (803) 777-9521. E-mail: ferry@mail.chem.sc.edu.

[†] University of South Carolina.

[‡] Coastal Center for Environmental Health and Biomolecular Research.

10.1021/jf072362x CCC: $37.00
Published on Web 10/31/2007

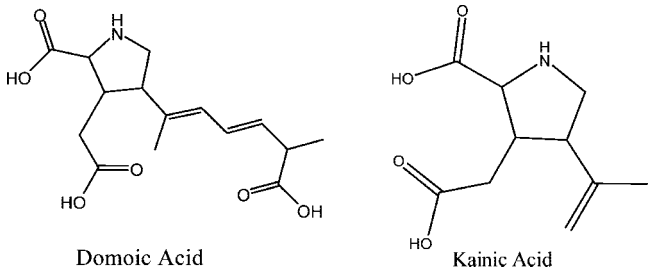

Figure 1. Structures of domoic and kainic acids.

Tables 2–5 in the Supporting Information). Domoic and kainic acids were obtained from EMD Biosciences, Inc. at 95% purity. $Fe_2(SO_4)_3 \cdot 5H_2O$ (97%) and $Cu(NO_3)_2 \cdot 2.5H_2O$ (98%) were purchased from Aldrich and used as received. Sodium nitrate (99%), sodium phosphate tribasic (99%), sodium bicarbonate (99%), benzoic acid (97%), sodium hydroxide (97%), and methanol [high-performance liquid chromatography (HPLC) grade[were obtained from Fisher Scientific. Deuterium oxide (D, 99.9%), sodium deuteroxide [D, 99.5%; NaOD, 30% (w/w) in D_2O], and deuterium chloride [D, 99.5%; DCl, 35% (w/w) in D_2O] were obtained from Cambridge Isotope Laboratories, Inc. NMR tubes were purchased from VWR and acid-cleaned before each use.

^{1}H Nuclear Magnetic Resonance (NMR) Spectroscopy. Proton NMR (500.211 MHz) spectra were collected on a Varian Inova 500 spectrometer with a 2.621 s acquisition time, 128 scans, 1 s recycle time, and a pulse width of 45° for 4.2 μs. Line width acquisition was obtained from unweighted transformed spectra using the standard deconvolution routine found in VNMR 6.1c software. Presaturation was used to suppress the dominant resonance of the residual water signal. Chemical shift referencing was done by assigning a nominal value of 4.6 ppm to the residual water signal. All spectra were collected at 25 °C and a digital resolution of 0.38 Hz. Because of possible binding of internal chemical-shift standards with Fe^{III}, chemical shifts reported herein and shown in the figures are approximate.

Kainic acid solutions (821 μM) were prepared and spiked with Fe^{III} or Cu^{II}, to yield a 1:1 kainic acid/metal molar ratio. D^+ activity was adjusted to a pD of 1.5 by the addition of 17.5% (w/w) DCl. NMR spectra were collected at pD increments of 0.2, ranging from 1.5 to 5.9. Additional spectra were collected at pD values of 6.15, 7.00, and 10.40. Kainic acid solution was quantitatively transferred from the NMR tube to a 5 mL conical-bottom vial between acquisitions, and pD was adjusted by the addition of concentrated NaOD while stirring. The solution was returned to the NMR tube, and the spectrum was collected. This process was repeated for each measurement.

Photodegradation Studies. Solar simulation was performed using a Suntest XLS+ Solar Simulator manufactured by Atlas Material Testing Solutions. Irradiation was achieved with the use of a 2200 W Xe vapor lamp, image broken by a diffuser, irradiating a 922.5 cm^2 polished stainless-steel surface. Light intensity was set to 655 W/m^2 (300–800 nm) with a coefficient of variation of 7.0% and 4.0 cm^2 resolution. Screw top borosilicate vials (2 mL), purchased from Laboratory Supply Distributors, served as photoreactors. Two 14.0 × 27.0 cm steel trays were used to hold 92 photoreactors each. Random distribution of the photoreactors avoided spatial bias from irregularities in the light field. All experiments were performed at a light intensity of 655 W/m^2 over a sample irradiation time of 15 h. The sample chamber temperature was controlled by an Atlas Suncool unit. The black standard temperature was 25–27 °C, with the chamber air temperature kept at 21 ± 2 °C. Seven reactors containing actinometer solution were randomly distributed among the set of 78 samples on each tray (*25*). All vials were airtight and perpendicular to the light source. All samples were stored in the dark before and after irradiation.

LC–MS/MS Analysis. Domoic and kainic acid samples were analyzed without any further sample treatment with an Agilent 1100 HPLC coupled to a Micromass-Quattro mass spectrometer equipped with an electrospray ion-spray (ESI) interface. Chromatographic separation was achieved using an Chromegabond WR C18 5 μm particle size, 15 cm × 2.1 mm (i.d.) column (ES Industries, West Berin, NJ)

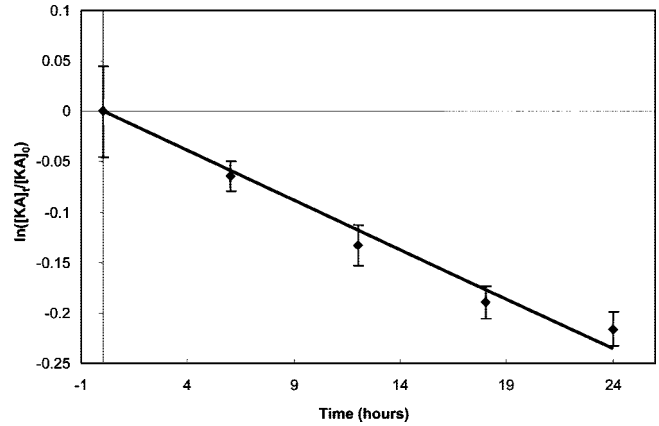

Figure 2. Plot of kainic acid degradation over time, $r^2 = 0.98$ (0.96 μM kainic acid, 32 ppt salinity, 5 mg/L DOM, 17.5 μM NO_3^-, 4 μM Fe^{III}, and 2 μM PO_4^{3-}). The $t_{1/2}$ of kainic acid under the above conditions is approximately 71 h.

in conjunction with a corresponding Chromegabond WR C18 5 μm particle size, 1 cm × 3.2 mm (i.d.) guard column. The LC–MS/MS procedure was as follows: A mixture of 0.1% aqueous formic acid in DI water (A) and 0.1% formic acid in acetonitrile (B) was used as the mobile phase. The initial condition was 95:5 A/B for 3 min, followed by a linear gradient over 13 min, ending at 5:95 A/B. The ratio of A and B was reset to the initial condition over the following 8 min to re-establish initial conditions. The flow rate was 200 μL/min, with a sample injection volume of 50 μL. A 5 min solvent diversion was used to avoid salt contamination of the ion source. The MS operating conditions were set to a cone voltage of 30 V, a collision voltage of 16 eV, a source block temperature of 100 °C, and a desolvation temperature of 350 °C. The mass spectrometer was run in multiple reaction monitoring mode (MRM), with a dwell time of 0.20 s. Domoic acid was identified and quantified by analysis of the signal from the parent mass (312.36 Da) and two daughter masses (266.10 and 161.30 Da), while kainic acid was identified and quantified using the parent mass of 214.00 Da and two daughter masses of 168.00 and 122.00 Da.

Direct cELISA Analysis. Analysis was performed using cELISA kits for ASP obtained from Biosense Laboratories, Bergen, Norway. Domoic acid/kainic acid samples were diluted 1:1 in extraction buffer (50% methanol in water) and added to activated DA-conjugated protein-coated plates at a dilution of 1:1 in sample buffer [10% methanol in phosphate-buffered saline (PBS)/0.05% Tween 20]. Polyclonal bovine anti-DA antibodies conjugated with a horseradish peroxidase (HRP) were used as free DA competitors. After 1 h of incubation, the samples were washed with unbound antibody (PBS/0.05% Tween 20). After this, a peroxidase substrate was added to react with the bound antibody, producing a blue product. The reaction was stopped using 0.3 M sulfuric acid. Samples were measured spectrophotometrically at 450 nm.

RESULTS AND DISCUSSION

Kainic acid has no appreciable absorbance in the solar spectrum and, therefore, does not undergo direct photolysis (0.96 μM kainic acid with 32 ppt salinity; see Supplementary Figure 1 in the Supporting Information). However, it was subject to indirect photodegradation, i.e., photodegradation resulting from the reaction with photogenerated transients from Fe^{III}, DOM, NO_3^-, etc. (**Figure 2**). The apparent loss was first-order in kainic acid (as indicated by analysis of $\ln([KA]_t/[KA]_o$ versus time). The observed rate constant (k_{obs}) was obtained by a linear least-squares analysis of the relationship between $[KA]_t/[KA]_o$ and time for all experimental conditions tested (**Table 1**). Half-lives for kainic acid ranged from 40 to 100 h. Shorter half-lives correspond to higher concentrations of added Fe^{III}. Speculatively, these results can be explained by analogy to the

Table 1. Rates of Kainic Acid Photolysis under Relevant Environmental Conditions[a]

run	DOM (mg/L)	Fe^{III} (μM)	NO_3^- (μM)	PO_4^{3-} (μM)	$k_{obs} \times 10^{-2}$ (h^{-1})	$t_{1/2}$ (h)	coefficient of variation
1	0.00	2.00	17.50	2.00	1.04	67.82	0.15
2	2.50	1.00	8.75	3.00	0.72	104.28	0.37
3	2.50	1.00	8.75	1.00	1.14	68.12	0.44
4	2.50	1.00	26.25	3.00	1.24	58.87	0.29
5	2.50	1.00	26.25	1.00	1.49	47.29	0.17
6	2.50	3.00	8.75	1.00	1.10	63.34	0.03
7	2.50	3.00	8.75	3.00	1.19	59.49	0.16
8	2.50	3.00	26.25	3.00	1.08	64.85	0.10
9	2.50	3.00	26.25	1.00	0.96	76.65	0.32
10	5.00	0.00	17.50	2.00	0.97	80.64	0.44
11	5.00	2.00	0.00	2.00	1.44	48.14	0.01
12	5.00	2.00	17.50	2.00	1.32	53.85	0.18
13	5.00	2.00	17.50	4.00	0.85	82.44	0.14
14	5.00	2.00	17.50	0.00	1.20	65.47	0.44
15	5.00	2.00	35.00	2.00	1.05	65.90	0.05
16	5.00	4.00	17.50	2.00	1.06	66.75	0.19
17	7.50	1.00	8.75	1.00	1.72	40.23	0.02
18	7.50	1.00	8.75	3.00	1.03	74.98	0.42
19	7.50	1.00	26.25	3.00	0.98	72.10	0.16
20	7.50	1.00	26.25	1.00	1.09	64.62	0.14
21	7.50	3.00	8.75	3.00	1.02	59.48	0.20
22	7.50	3.00	8.75	1.00	1.52	46.93	0.21
23	7.50	3.00	26.25	3.00	1.14	66.81	0.39
24	7.50	3.00	26.25	1.00	1.12	63.09	0.19
25	10.00	2.00	17.50	2.00	1.19	59.48	0.17

[a] All samples contain 0.96 μM kainic acid along with 32 ppt salinity.

photodegradation of domoic acid in the presence of Fe^{III}, where a signficant fraction of domoic acid loss was through the photolysis of a DA/Fe^{III} complex.

The possibility of such a complex was explored through the application of a ^{1}H NMR titration technique similar to that used to characterize the DA–Fe^{III} complex (*12*). The NMR spectrum of kainic acid (see Supplementary Figure 2 in the Supporting Information) in the presence or absence of metal (Fe^{III} or Cu^{II}) was obtained at varying pD values (pD 1.5–12.0). The analytical observation for the experiment was the line width at half-height for the ^{1}H NMR spectrum of kainic acid at 1.8 ppm (a singlet derived from the methyl group α to the pyrrolidine ring; see Supplementary Figure 2 in the Supporting Information). At low pD (1.5), line widths were the same for spectra taken with and without metal, indicating that kainic acid and the metal were not associated (**Figures 3** and **4**) (*26*). Line widths broadened rapidly as pD increased in both the Fe^{III} and Cu^{II} samples but remained essentially unchanged in the sample with kainic acid alone. At low pD, metal concentrations were not high enough to cause line broadening (a through space effect), with line broadening at higher pD values a consequence of complexation. The titration curve obtained from plotting line width versus pD demonstrated two inflection points at pD 3.38 and 5.50 for the Fe^{III}–KA complex and pD 4.50 and 6.00 for the Cu^{II}–KA complex, suggesting that the resulting complexes have a 2:1 stoichiometry (KA/metal). This behavior is consistent with that of other natural and artificial amino acids with pH-dependent K' [e.g., glutamic acid and ethylenediaminetetraacetic acid (EDTA)] that complex metals strongly in the deprotonated form but only very weakly in acidic environments (*27*, *28*). Association constants, K, for the KA/Fe^{III} complex were estimated on the basis of the assumption that kainic acid, similar to other amino acids, complexes metals most effectively in the fully deprotonated (Y^{3-}) form (*27*). On the basis of the position of the inflection point, measured pK_a values were as follows: pK_{a_1} = 1.96, pK_{a_2} = 6.02, and pK_{a_3} = 10.80 (see Supplementary Figure 3 in the Supporting Information) and the initial concentrations of Fe^{III} and kainic acid were as follows: the estimated value of K_1 was 2.27×10^{12} and the estimated value of K_2 was 8.99×10^8. The estimated stability constants for the KA/Cu^{II} complex are $K_1 = 1.38 \times 10^{10}$ and $K_2 = 4.35 \times 10^7$. The binding constants reported here were corrected for competitive binding of the metal to OH^-, Cl^-, and SO_4^{3-}/NO_3^-, which were present in the titrated solution and also corrected for pH (see Supplementary Calculation 1 in the Supporting Information) (*29*–*32*). These results indicate that, under the conditions of our photodegradation experiments, essentially all kainic acid was bound to a transition metal.

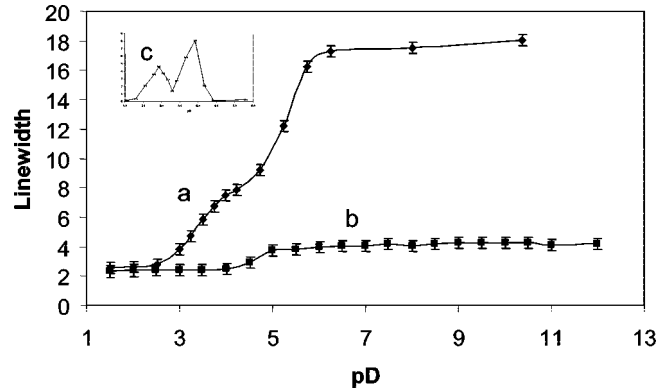

Figure 3. (a) As pD increased, the line width of the singlet at 1.8 ppm increased in the presence of Fe^{III}, implying the formation of a complex. [Kainic acid] = 821 μM; [Fe^{III}] = 821 μM; and DCl and NaOD were used for pD adjustment. (b) As pD increases, the line width of the singlet at 1.8 ppm remains the same for KA alone. (c) First derivative plot for inflection point assignment.

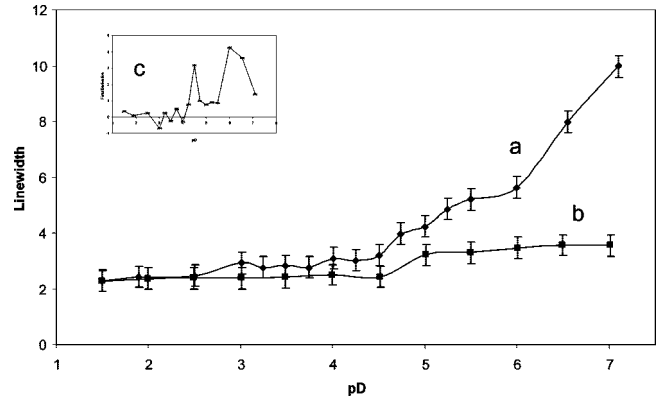

Figure 4. (a) As pD increased, the line width of the singlet at 1.8 ppm increased in the presence of Cu^{II}, implying the formation of a complex. [Kainic acid] = 821 μM; [Cu^{II}] = 821 μM; and DCl and NaOD were used for pD adjustment. (b) As pD increases, the line width of the singlet at 1.8 ppm remains the same for KA alone. (c) First derivative plot for inflection point assignment.

These constants are of the same order as those obtained for the association of Fe^{III} and domoic acid, which may co-occur with kainic acid in some marine algae (*12*, *13*). Accordingly, a series of competitive photodegradation experiments were performed to test the relationship between the magnitude of K and the photodegradation rate of either acid. Domoic acid quickly photodegraded over the time period of the experiment and under the conditions tested (**Table 2**). It was found that domoic acid half-lives ranged from 12 to 34 h, depending upon the experimental conditions. A comparison of half-lives of KA in the presence of DA showed that half-lives for KA in mixed solutions are ~4 times longer than when KA is photodegraded alone (5.00 mg/L DOM, 2 μM Fe^{III}, 17.50 μM NO_3^-, and 2.00

Table 2. Comparison of the Half-Lives Found Using LC–MS/MS and cELISA To Quantify Domoic Acid[a]

run	[DOM] (mg/L)	[Fe^{III}] (μM)	[NO_3^-] (μM)	[PO_4^{3-}] (μM)	predicted DA $t_{1/2}$ (h)	average KA $t_{1/2}$ (h) (LC–MS/MS)	average DA $t_{1/2}$ (h) (LC–MS/MS)	coefficient of variation for LC–MS/MS	average DA $t_{1/2}$ (h) (cELISA)	coefficient of variation for cELISA
1	10.00	0.00	0.00	0.00	20.09	256.72	21.31	0.11	38.06	0.32
2	0.00	4.00	0.00	0.00	15.98	42.52	8.81	0.69	47.47	0.31
3	0.00	0.00	35.00	0.00	35.26	866.43	47.05	0.24	81.20	0.25
4	0.00	0.00	0.00	4.00	26.72	577.62	49.39	0.18	84.77	0.10
5	0.00	2.00	17.50	2.00	25.21	106.64	36.48	0.64	32.73	0.32
6	5.00	0.00	17.50	2.00	21.89	88.87	29.66	0.08	24.00	0.20
7	5.00	2.00	0.00	2.00	16.92	301.37	82.85	0.34	50.43	0.16
8	5.00	2.00	17.50	0.00	15.59	101.93	21.42	0.31	42.49	0.19
9	5.00	2.00	17.50	1.00	16.16	198.04	26.16	0.28	41.26	0.12
10	5.00	2.00	17.50	2.00	16.50	210.04	33.16	0.36	41.32	0.15
11	5.00	2.00	17.50	3.00	16.59	231.05	26.26	0.14	60.54	0.26
12	5.00	2.00	17.50	4.00	16.40	1155.25	26.52	0.03	35.09	0.19
13	0.00	0.00	0.00	0.00	84.32	192.54	90.81	0.50	144.54	0.19

[a] All samples contain 0.96 μM domoic and kainic acid along with 32 ppt salinity.

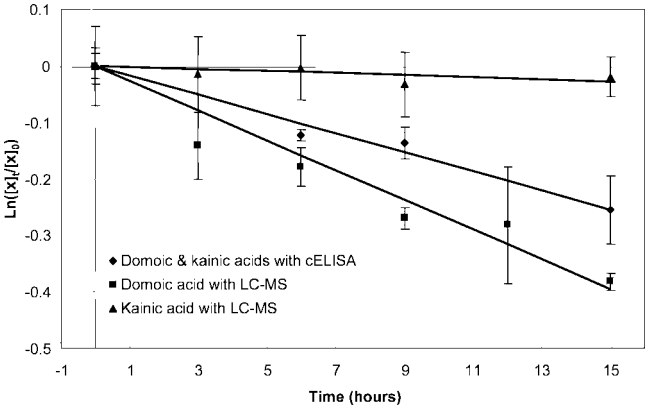

Figure 5. Typical plot of toxin degradation over time (0.96 μM domoic acid, 0.96 μM kainic acid, 32 ppt salinity, 5 mg/L DOM, 17.5 μM NO_3^-, 2 μM Fe^{III}, and 1 μM PO_4^{3-}). The domoic acid quantified using the cELISA technique is ~1.5 slower than the rate found using LC–MS (domoic and kainic acids with cELISA, $r^2 = 0.98$; domoic acid with LC–MS/MS, $r^2 = 0.95$; and kainic acid with LC–MS/MS, $r^2 = 0.001$).

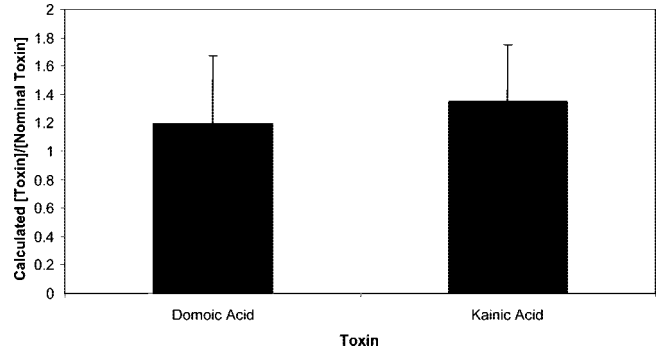

Figure 6. Comparison of the relative concentrations of domoic and kainic acids, as calculated from the cELISA test. When the toxins were run separately, there was a 1:1 response on the cELISA for kainic acid. The conditions are 0.96 μM toxin and 32 ppt salinity, with $n = 6$ replicates.

μM PO_4^{3-}). The implication is that these acid–metal complexes may become labile after photoreduction of the Fe^{III}, allowing catalytic cycling of Fe^{III}.

In addition to monitoring the molecular composition of the photodegraded mixture by LC–MS/MS techniques, the toxicity of the resulting mixture was assayed using a cELISA assay (BioSense Laboratories) designed to measure the domoic acid response alone. The response was plotted ($\ln([x]_t/[x]_0)$ versus time) to determine the rate (k_{obs}) of domoic acid photodegradation in the presence of kainic acid (**Figure 5**). When this result was indexed against the predicted k_{obs} for these conditions (on the basis of a multifactorial model, incorporating the effects of Fe^{III}, DOM, PO_4^{3-}, and NO_3^-) (*12*), the cELISA routinely underpredicted the rate of domoic acid loss relative to the MS-based method. Although the degree of underprediction varied with experimental conditions, the difference between the two analytical methods was consistently significant to the 99% level of confidence. There was no correlation between the degree of underprediction and the rate of reaction, indicating that underprediction was a function of kainic acid–assay interactions and not attributable to possible photoproducts (*3*, *4*, *7*). This interaction was tested by exposing the assay to both prepared standards of kainic and domoic acids and measuring the response. A comparison of the apparent concentrations yielded a 1:1 ratio of domoic acid/kainic acid (**Figure 6**; see Supplementary Table 6 in the Supporting Information). Together, these results indicated that (1) the cELISA was approximately as sensitive to kainic acid as domoic acid, (2) the cELISA kits overestimate domoic acid in the presence of kainic acid, and (3) photoproducts did not elicit a response from the assay.

ACKNOWLEDGMENT

The authors thank Perry Pellechia for his help with the NMR.

Supporting Information Available: Supplementary Tables 1–6, Supplementary Figures 1–3, and Supplementary Calculation 1. This material is available free of charge via the Internet at http://pubs.acs.org.

LITERATURE CITED

(1) Sato, M.; Nakano, T.; Takeuchi, M.; Kanno, N.; Nagahisa, E.; Sato, Y. Distibution of neuroexcitatory amino acids in marine algae. *Phytochemistry* **1996**, *42* (6), 1595–1597.

(2) Higa, T.; Kuniyoshi, M. Toxins associated with medicinal and edible seaweeds. *J. Toxicol., Toxin Rev.* **2000**, *19* (2), 119–137.

(3) Madhyastha, M. S.; Novaczek, I.; Ablett, R. F.; Johnson, G.; Nijjar, M. S.; Sims, D. E. In vitro study of domoic acid uptake by digestive gland tissue of bule mussle (*Mytilus edulis* L.). *Aquat. Toxicol.* **1991**, *20* (1–2), 73–81.

(4) Madhyastha, M. S.; Novaczek, I.; Ablett, R. F.; Johnson, G.; Nijjar, M. S.; Sims, D. E. A comparative study of uptake and release of glutamic-acid and kainic acid by blue mussel (*Mytilus edulis* L.). *Aquat. Toxicol.* **1991**, *21* (1–2), 15–28.

(5) Trainer, V. L.; Bill, B. D. Characterization of a domoic acid binding site from Pacific razor clam. *Aquat. Toxicol.* **2004**, *69*, 125–132.

(6) Sperk, G.; Lassmann, H.; Baran, H.; Kish, S. J.; Seitelberger, F.; Hornykiewicz, O. Kainic acid induced seizures: Neurochemical and histopathological changes. *Neuroscience* **1983**, *10* (4), 1301–1315.
(7) Hampson, D. R.; Manalo, J. L. The activation of glutamate receptors by kainic acid and domoic acid. *Nat. Toxins* **1998**, *6*, 153–158.
(8) Doucette, T. A.; Strain, S. M.; Allen, G. V.; Ryan, C. L.; Tasker, R. A. R. Comparative behavioural toxicity of domoic acid and kainic acid in neonatal rats. *Neurotoxicol. Teratol.* **2000**, *22*, 863–869.
(9) Goldberg, J. D. Domoic acid in the bethic food web of Monterey Bay, CA. Masters Thesis, CA State University Monterey Bay, Monterey Bay, CA, 2003.
(10) van Dolah, F. M. Marine algal toxins: Origins, health effects, and their increased occurrence. *Environ. Health Perspect.* **2000**, *108* (S1), 133–141.
(11) van Dolah, F. M.; Doucette, G. J.; Gulland, F. M. D.; Rowles, T. L.; Bossart, G. D. Impacts of algal toxins on marine mammals. In *Toxicology of Marine Mammals*; CRC Press: Boca Raton, FL, 2003; pp 247–269.
(12) Fisher, J. M.; Reese, J. G.; Pellechia, P. J.; Moeller, P. L.; Ferry, J. L. Role of Fe(III), phosphate, dissolved organic matter, and nitrate during the photodegradation of domoic acid in the marine environment. *Environ. Sci. Technol.* **2006**, *40* (7), 2200–2205.
(13) Rue, E.; Bruland, K. Domoic acid binds iron and copper: A possible role for the toxin produced by the marine diatom *Pseudo-nitzschia*. *Mar. Chem.* **2001**, *76*, 127–134.
(14) Wells, M. L.; Trick, C. G.; Cochlan, W. P.; Hughes, M. P.; Trainer, V. L. Domoic acid: The synergy of iron, copper, and the toxicity of diatoms. *Limnol. Oceanogr.* **2005**, *50* (6), 1908–1917.
(15) Bates, S. S.; Leger, C.; Wells, M. L.; Hardy, K. In *Photodegradation of Domoic Acid*, Proceedings of the Eighth Canadian Workshop on Harmful Marine Algae, Moncton, New Brunswick, Canada, May 28–30, 2003; Bates, S. S., Ed.; Fisheries and Oceans Canada: Moncton, New Brunswick, Canada, 2003; pp 30–36.
(16) Trainer, V. L.; Hickey, B. M.; Horner, R. A. Biological and physical dynamics of domoic acid production off the WA coast. *Limnol. Oceanogr.* **2002**, *47* (5), 1438–1446.
(17) Bouillon, R. C.; Knierim, T. L.; Kieber, R. J.; Skrabal, S. A.; Wright, J. L. C. Photodegradation of the algal toxin domoic acid in natural water matrices. *Limnol. Oceanogr.* **2006**, *51* (1), 321–330.
(18) U.S. Department of the Interior, United States Geological Survey (USGS). National Water Information System: Web Interface In USGS Publishing Network, 2005.
(19) Bruland, K. W.; Rue, E. L.; Smith, G. J. Iron and macronutrients in CA coastal upwelling regimes: Implications for diatom blooms. *Limnol. Oceanogr.* **2001**, *46* (7), 1661–1674.
(20) Hallegraeff, G. M. A review of harmful algal blooms and their apparent global increase. *Phycologia* **1993**, *32* (2), 79–99.
(21) Hoppe, H.-G. Phosphatase activity in the sea. *Hydrobiologia* **2003**, *493*, 187–200.
(22) Maldonado, M. T.; Hughes, M. P.; Rue, E. L.; Wells, M. L. The effect of Fe and Cu on growth and domoic acid production by *Pseudo-nitzschia*. *Limnol. Oceanogr.* **2002**, *47* (2), 515–526.
(23) Trainer, V. L.; Adams, N. G.; Bill, B. D.; Stehr, C. M.; Wekell, J. C.; Moeller, P.; Busman, M.; Woodruff, D. Domoic acid production near CA coastal upwelling zones, June 1998. *Limnol. Oceanogr.* **2000**, *45* (8), 1818–1833.
(24) Otero, E.; Culp, R.; Noakes, J. E.; Hodson, R. E. The distribution and $\delta^{13}C$ of dissolved organic carbon and its humic fraction in estuaries of southeastern USA. *Estuarine, Coastal Shelf Sci.* **2003**, *56*, 1187–1194.
(25) Jankowski, J. J.; Kieber, D. J.; Mopper, K. Nitrate and nitrite ultraviolet actinometers. *Photochem. Photobiol.* **1999**, *70* (3), 319–328.
(26) Bloembergen, N.; Purcell, E. M.; Pound, R. V. Relaxation effects in nuclear magnetic resonance absorption. *Phys. Rev.* **1948**, *73*, 679–712.
(27) Harris, D. C. *Exploring Chemical Analysis*, 2nd ed.; W. H. Freeman and Company: New York, 2001.
(28) Micklitsch, C. M.; Yu, Q.; Schneider, J. P. Unnatural multidentate metal ligating α-amino acids. *Tetrahedron Lett.* **2006**, *47*, 6277–6280.
(29) Glasoe, P. K.; Long, F. A. Use of glass electrodes to measure acidities in deuterium oxide. *J. Phys. Chem.* **1960**, *64*, 188–190.
(30) DeCoursey, T. E.; Cherny, V. V. Deuterium isotope effects on permeation and gating of proton channels in rat alveolar epithelium. *J. Gen. Physiol.* **1997**, *109*, 415–434.
(31) Hogfeldt, E. *Stability Constants of Metal–Ion Complexes. Part A: Inorganic Ligands*; Pergamon Press: New York, 1982.
(32) Millero, F. J.; Yao, W.; Aicher, J. The speciation of Fe(II) and Fe(III) in natural waters. *Mar. Chem.* **1995**, *50*, 21–39.

Received for review August 6, 2007. Revised manuscript received September 26, 2007. Accepted September 28, 2007. This work was supported by the U.S. Environmental Protection Agency (EPA) Grant RD83-1042.

JF072362X